Journal of Materials Processing Technology 164–165 (2005) 1140–1147

Journal of Materials Processing Technology

www.elsevier.com/locate/jmatprotec

Experimental and numerical simulation of tube hydroforming (THF)

J.P. Abrantes, A. Szabo-Ponce, G.F. Batalha *

Department of Mechatronics and Mechanical Systems Engineering, Polytechnic School, University of S. Paulo, Av. Prof. Mello Moraes 2231, 05508.900 Sao Paulo, SP, Brazil

Abstract

Hydroforming is a manufacturing process that uses a fluid medium to form a part by using high internal pressure. In tube hydroforming (THF), a tubular blank is placed between two dies, sealed and filled by injecting pressurized water up to 1200 MPa into it, deforming its walls and calibrating them to shape the die cavities. The advantages of the hydroforming over the traditional process are: (a) light weight constructions; (b) design flexibility increase, enable new shapes; (c) stiffness increase by using no welded tubular blanks; (d) welded assembly elimination; (e) dimensional accuracy. The weight reduction obtaining by THF can be aided by further reduction trough lighter materials selection. This paper aims to establish a basic understanding of the THF processing of aluminum and copper tubes. The THF is briefly reviewed by carrying out an FEA of 2 THF processes. The first simulation case is the THF of a free aluminum tube without thrust feed force. The second one is a study of THF calibration into a closed die. Finally, some preliminary results on the design and development of THF facility as well as its control are presented with some experimental results, looking for a THF process window.

Keywords: Hydroforming; Plasticity; Tube; Aluminum; FEM; Wrinkling

1. Introduction

The tube hydroforming processes (THF) consist of a combined loading of compression forces (thrust and radial) as well as an internal pressure (applied by a fluid media) in order to obtain tubular components with different cross-sections. THF is manufacturing process used mainly to produce low cost and lightweight components, maintaining their structural integrity, compared with traditional forming processes [1–11]. Nowadays, two THF techniques outstand: the THF with sequenced pressurization (PSH) and the high pressure hydroforming (HPH). Both approaches were developed to make easier the THF of more complex parts, avoiding problems such as wrinkling, buckling and rupture. However the name, emphasizing the pressure behavior difference, the true difference between the two techniques is not the way to apply the pressure, but the way the tubular blank is positioned into the dies. The final pressure results of the mounted tool set. It should take care to do not make mess between the pressure level and the forming potential of the hydroformed part aiming to obtain a perfect part.

In the first part of this work, it is analyzed a free expansion tube hydroforming that does not regard any aspect of the pressure applying pressure, once it did not regard the die reactions forces. However, the attained pressure level could be regarded as a HPH process. More details are discussed in [4]. This paper aims under base of former works on sheet metal bulging [6,7], to begin a study both THF with radial loading on a free expansion without calibrating dies, as well THF using calibrating die tool sets. In this sense, as a first approach, it is intended to calibrate the software LS-DYNA as well as the numerical model and analysis, using own results and former results from the literature [5,8].

2. Free bulging THF

After [3], the theoretical pressure necessary to start the THF bulging process can be determined by the following expression:

$$p_0 = \frac{\sigma_y t}{r} \quad (1)$$

where σ_y is the yield stress of the tube material, t the thickness of the tube wall and r the average radius of the tube. The exper-

* Corresponding author.
E-mail address: gilmar.batalha@poli.usp.br (G.F. Batalha).

0924-0136/$ – see front matter © 2005 Elsevier B.V. All rights reserved.
doi:10.1016/j.jmatprotec.2005.02.117

Table 1
Tube blank model for the tube blank

Material	AA6082-T4
Thickness, t (mm)	3.175
Average radius, r (mm)	17.4625
Length, L (mm)	240
Density, ρ (g/cm^3)	2.7
Young modulus, E (GPa)	71
Poisson coefficient, ν	0,31
Strength factor, K (MPa)	550
Strain hardening exponent, n	0.25
Yield stress, σ (MPa)	160

imental material use on this simulation is an aluminum alloy AA6082-T4, already related by [1]. Its mechanical properties are resumed in Table 1. After the data in Table 1, it is determined for THF free bulging to be simulated in this work, a pressure: $p_0 = 29.1$ MPa.

2.1. FEM model for the free bulge THF

For the free bulging THF simulation it was used the software LS-DYNA for non-linear FEA [12]. The die was modeled with solid elements. The material model for the tubes was the model 36 (MAT_3-PARAMETER_BARLAT) with Lankford parameter stated as 1, regarding an isotropic material and exponential strain hardening law (Holomon), $\sigma = K\varphi^n$. The final model contains 258 nodes and 205 elements. It was assumed a lubricated condition between the die and tube, by using a Coulomb model, with friction coefficient $\mu = 0.05$. Table 1 resumes the model data and Fig. 2 represents the model generated.

2.2. Boundary conditions and FEA of the free bulging THF

Due to the symmetry conditions of the model, it was modeled only 1/8 of the tube blank, regarding three symmetry planes, following the application of the necessary boundary conditions on the nodes of the tube model. The ends of the tube blank are free and slide along its axle. Fig. 1 shows the model and Fig. 2 shows its respective boundary conditions.

2.3. FEM procedure and free bulge THF results

At a first glance there are two methods for the pressure application: a linear method and the bilinear one. Both methods involve high pressure loading rates, regarding its physical effects. In this work, the pressure loading rate was accelerated to a maximum in order to reduce the computing time, however using internal and kinetic energy control, in order to do not disturb the physical meaning of the a real THF process. The loading cycle is showed in Fig. 3. The adopted material model did not include failure criteria after uniform strain step, represented by the Holomon equation $\sigma = K\varphi^n$ aiming

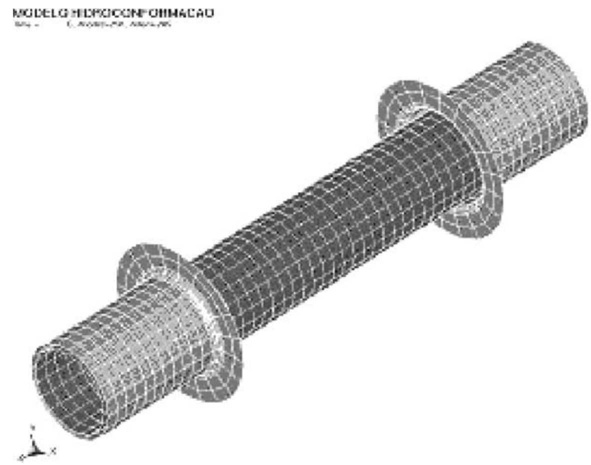

Fig. 1. FEM model.

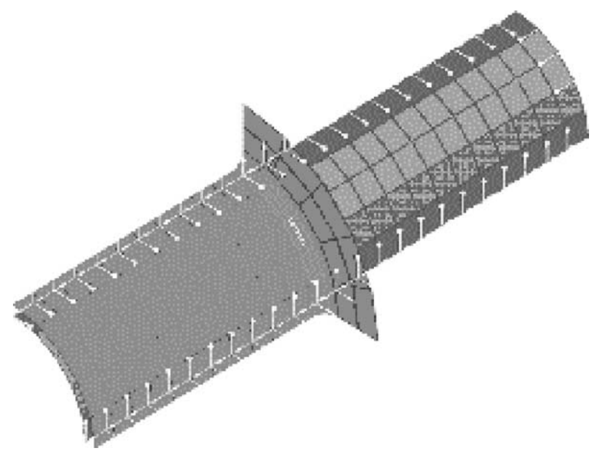

Fig. 2. FEM boundary conditions.

the identification of the necking begin. In order to do this, it was used a limit strain based failure criterion. It was assumed that failure occurs when the plastic strain reaches 10%, basing this value on the FLD curve presented in [5]. Regarding the increase in radius or bulge height, Fig. 4 presents the maxi-

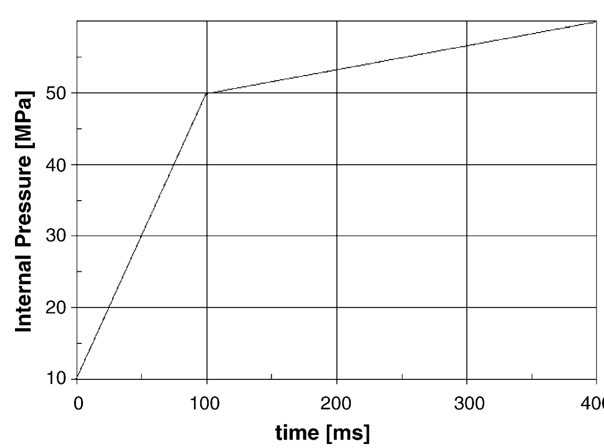

Fig. 3. Curve internal pressure vs. time.

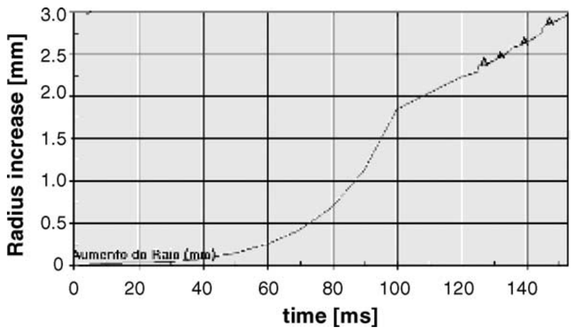

Fig. 4. Tube radius or height increase vs. time.

mal displacement (bulge height) versus the time until the tube rupture. From this figure, it is concluded that the bulge height for a time $t = 110$ ms reaches 2.05 mm, which is in agreement with [5].

Based on the assumed failure criterion, it was obtained the burst pressure (Fig. 5) for simulation stated as 50.3 MPa, which represents an error of 3.5% from value obtained by [5]. Fig. 6 presents the thickness distribution on the hydroformed part. The critical moment of the tube bursting presents a maximal reduction of 5.25% in the tube wall thickness. Table 2 resumes the results of FEA compared results.

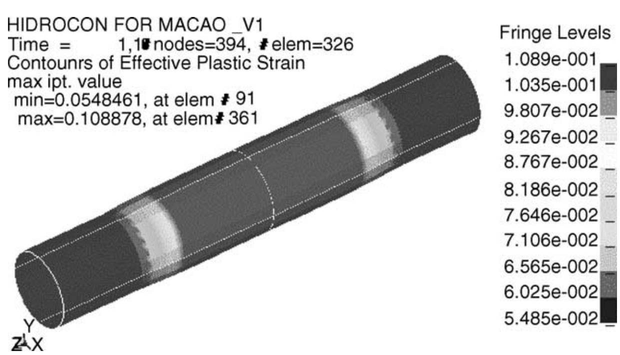

Fig. 5. Effective strains on the 6082-T4 tube, $t = 110$ ms ($\varepsilon = 0.109$), $p = 50.3$ MPa.

Fig. 6. Thickness distribution for the 6082-T4 tube.

Table 2
Compared results of the FEA for the THF model

	This work	Ref. [5]	Error
Burst pressure (MPa)	50.33	47.7–49.8	0.35%
Bulge height (mm)	2.05	1.52–2.29	∼0
Min. thickness (mm)	2.97	–	–

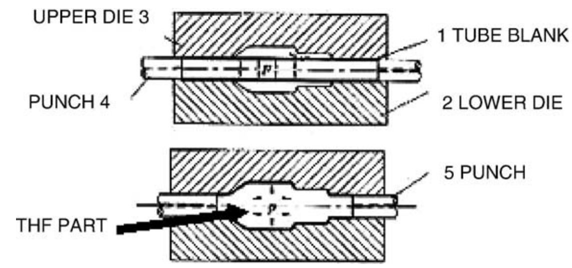

Fig. 7. THF calibration process into closed dies.

3. THF calibration process with closed dies

The study of THF calibration process in this work, took as reference the earlier approach of [8]. Fig. 7 presents a brief description of the modeled process.

At the begin, the tube blank 1 is positioned into the lower die cavity, with further step of closing the die set, aiming to avoid the movement of the tube blank. In the following step, the tube is filled with a liquid medium through a feed hole in the punch and it is applied an initial pressure. In the next steps, the punches 4 and 5 are moved in order apply a thrust force at the ends of the tube. Depending on the combined effect of the thrust force feeding and the internal pressure loading synchronization, this operation results in tube buckling, as well as also wrinkling. After the punch reaches the programmed stroke displacement the internal pressure on the fluid into the tube is increased expanding the tube, in such a way that it took the forms of the die cavity. This operation is the so called calibration. In general terms, there is process window where is to be combined the thrust feeding force with internal pressure, in order to obtain hydroformed parts without wrinkles or tearing. The wrinkles generated during the buckling in the THF process could be bad or good ones. Recent works [8–11] outstand the wrinkles produced in the buckling stage could be distinguished as good or bad ones, and they are related to determined combination of punch stroke and initial internal pressure sets. The wrinkle would be a benefic one if it can be completely removed in the calibration step, otherwise the bad one will still be after the calibration step. The determination of the most suitable combination of thrust feed force and initial internal pressure is to be analyzed by an FEA approach described in the following section.

3.1. FEA data and boundary conditions THF calibration

The THF calibration process into closed dies was carried out based on the geometry studied earlier by [8]. For this specific tube geometry the THF process became more suitable

Table 3
Geometry data and properties of the THF blank (material: aluminum alloy LF2M)

Tube diameter (mm)	65
Tube length (mm)	250
Thickness (mm)	1.5
Yield stress (GPa)	0.08
Strength coefficient, K (GPa)	0.6
Density, ρ (g/cm^3)	2.7
Young modulus, E (GPa)	71
Poisson coefficient, ν	0.31
Strain hardening coefficient, n	0.25
Friction coefficient, μ	0.125

due to its initial and final diameter ratio. The tube starts from an initial diameter of 65 mm that reaches a diameter for a final hydroformed part of 88 mm, resulting in an elongation of 33.4%. Keeping a ratio between the length of the expansion zone at axial direction ($100 + 2 \times (31.6) = 163.2$ mm) and the tube diameter, equal to 2.5. Such ratio turns impossible to form this by a traditional process of hot drawing of tubes. Table 3 resumes the necessary data for the FEA of the THF process.

The parameter setting for the thrust feeding force as well as the internal pressure behavior during the THF process was made regarding the parameters setting suggested by [8]. They indicate that a minimal internal pressure should be applied to the tube blank in order to obtain a part without winkles are to be 5.5 MPa. It was taken as reference steps the pressures of 0, 3 and 5 MPa, and punch strokes above 15 mm, remembering that for all these conditions the earlier simulation results predicted wrinkles in the final calibration stage. These examples were regarded aiming the development of an FEM model implemented with the commercial FEM software LS-DYNA (the modelling approaches are presented in Figs. 8 and 9). Those models are to be calibrated with the reported results for the three internal pressures magnitudes, discussed in the following sections.

3.2. FEA results for the THF calibration

Fig. 10 shows the results for the internal pressures 0.0, 3.0 and 5.5 MPa, all of them for a punch stroke of 15 mm. Analysing the results in terms of process window postulated

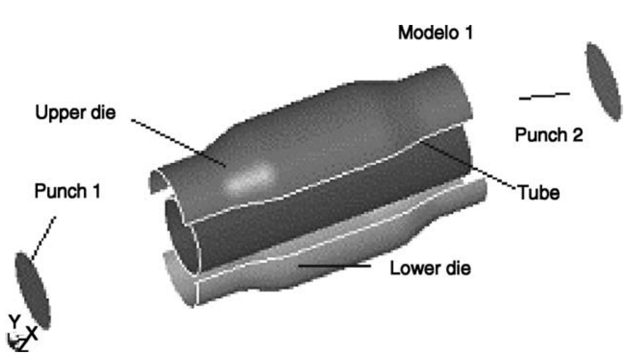

Fig. 8. FEM model 1 for the THF calibration.

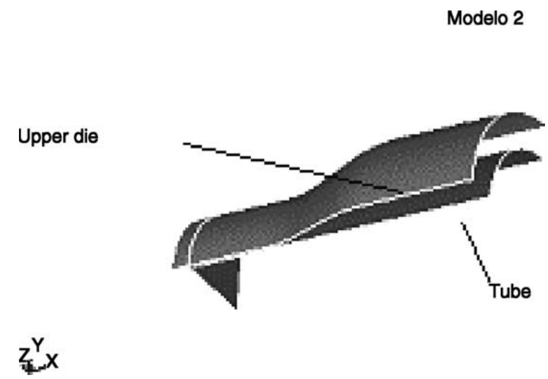

Fig. 9. FEM model 2 for the THF calibration.

by [8], the simulation results agree with his results and comproves the quality of the developed model and analysis.

4. Development of a THF system and its control for T part

Under basis of some earlier experiences [13–17] a hydroforming unit and its control were developed during this work. Its development and control aim to avoid the main defects presented in a hydroformed part (Fig. 11). The control is based on the FEA simulation and demands of a better control for THF process window; accounting the thrust feed force and the internal pressure (Fig. 12).

A hydroforming unit for THF was specially designed for T branch parts. It includes the spliced die set, one counter pressure punch and one closing punch, two independent hydraulic units, one to feed the punch cylinders and the second one to feed the pressurized fluid into the hydroformed part. The systems control includes also common and proportional directional valves, servovalves and sensors. The diagrams illustrated in Figs. 13 and 14 represent the hydraulic system configuration.

In the diagram showed in Fig. 13 it can be noted two different hydraulic units, where the symbol AX stays for axial cylinders, CP for counter pressure, F for closing, AP for the pressure amplifier, UH1 for the main hydraulic unit, UH2 for hydraulic unit of the pressure booster system. The two units are detailed in Figs. 14 and 15.

Fig. 14 illustrates the basic hydraulic unit, the closing cylinder, responsible for the die closing, which is controlled by a directional flow valve, manually operated by a button key. Also in this figure, it can be observed that axial cylinders those actuate the two thrust feed forces, are controlled each one by a proportional flow valve. The counter pressure valve equipped with a load cell is controlled by a common directional valve, aided by manual flow controls.

Fig. 15 shows the amplifier pressure booster composed by a servo actuator and a servo valve, with capacity to supply internal pressure up to 210 bar. Finally Fig. 16 schematizes the feed back control option choused for the control and

Fig. 10. FEA evolution for the THF calibration stages (time in ms).

data acquisition systems implemented in the THF facility. Figs. 17 and 18 show the use of PCI circuits to control the different components. Finally Fig. 19 shows the images of the main components of the THF unit constructed.

The control systems as well the stroke and valves movement is discussed elsewhere [21–23]. If the cylinders stroke were not so close, the hydroformed T branch presents two defects: the bulge is not centralized (Fig. 20); trend to form a bulge with different lateral slopes, bigger slope at side with greater velocity (Fig. 21). It could be viewed in Fig. 20 that the bulge at its beginning is not centralized. The side marked has displaced with more velocity that the other side. Fig. 21 shows a part with wrinkling (the wrinkles are emphasized with the black darts), that denotes an excessive axial feed

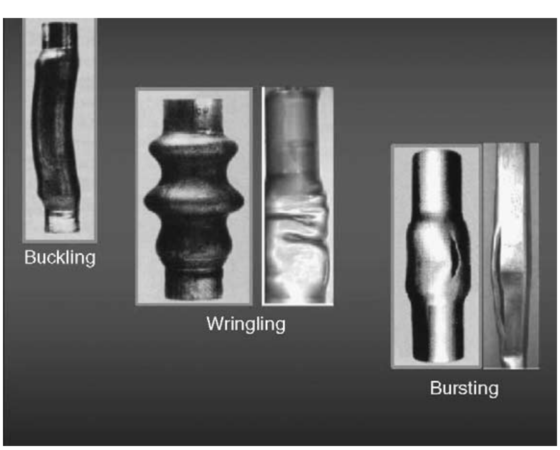

Fig. 11. Main defects on THF process [18].

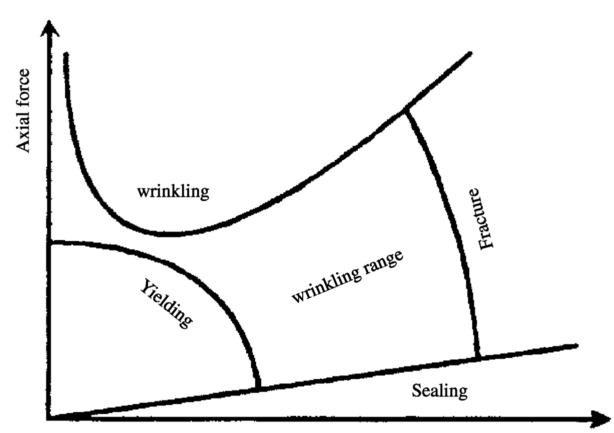

Fig. 12. Example of THF process window [19,20].

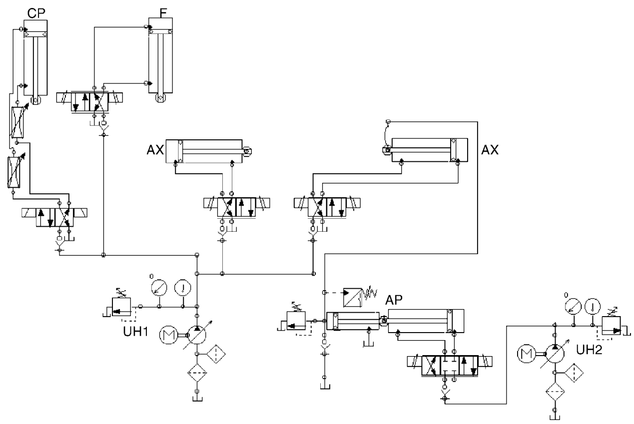

Fig. 13. Simplified THF general hydraulic diagram.

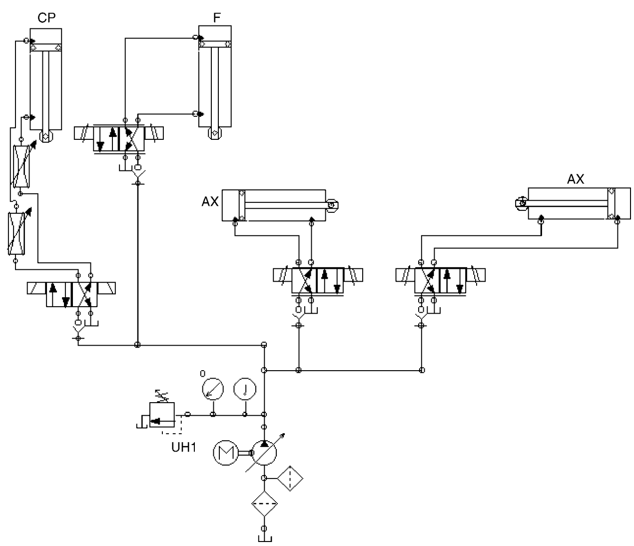

Fig. 14. The basic hydraulic unit diagram.

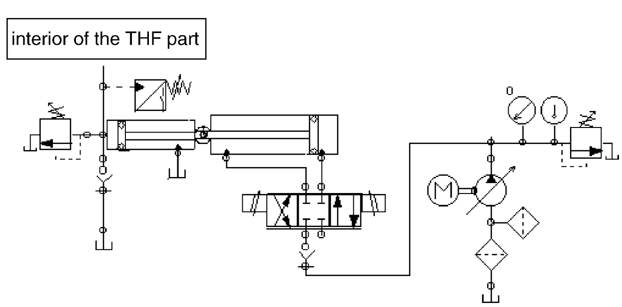

Fig. 15. Pressure amplifier unit hydraulic diagram.

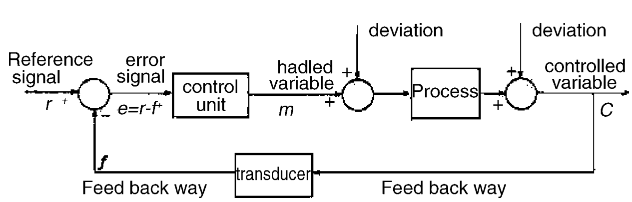

Fig. 16. Feed back control mode.

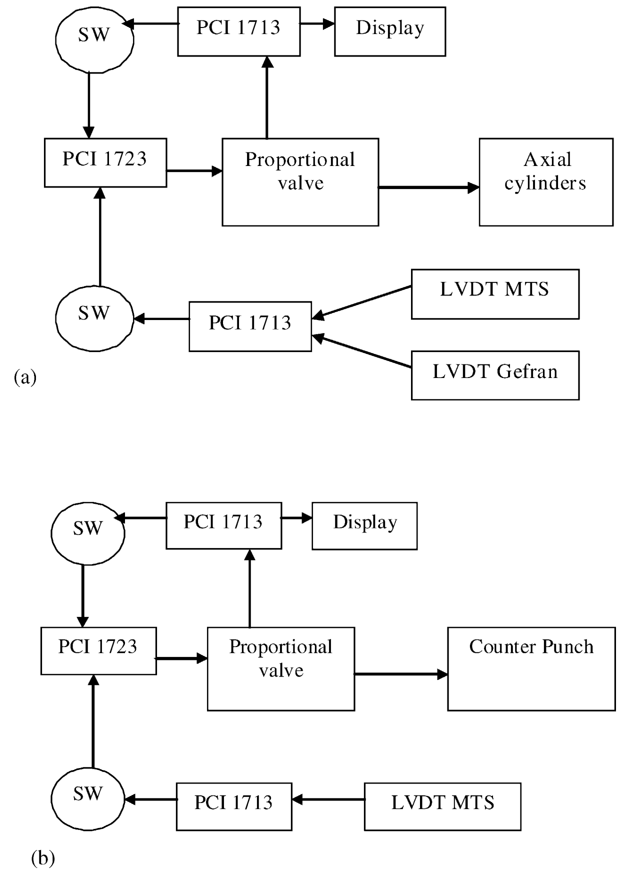

Fig. 17. Reading and writing routes for sensors and actuators: (a) axial cylinders; (b) counter punch.

compression compared with the increasing of the internal pressure into the tube. It is also observed the trend of a bulge slope at the side deformed with more velocity. In Fig. 22 it could be observed that in this specimen suffered a fracture due to an excessive internal pressure, followed by a buckling collapse after the depressurization.

5. Conclusions and future perspectives

This work used the FEA program LS-DYNA for a successful FEM model for both free bulge and calibration against closed dies THF processes. It obtains results that agree with earlier analysis of the literature, presenting no significant errors.

The success of this first calibration step for the LS-DYNA based model, allows for the beginning of the next steps, which preview the study of the hydroforming process for more complex geometry of parts, typical for industrial cases.

For the THF calibration process against closed dies, the formation of benefic winkles, resulting in folding and unfolding of tube regions, causes a differenced spring back effect along the longitudinal axle of the tube, that results in distortion in hydroformed part after its withdraw from the die.

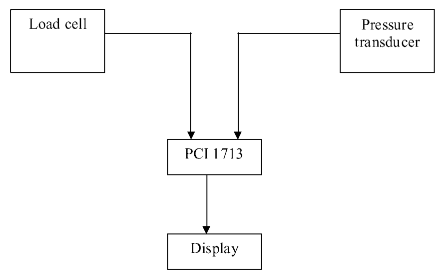

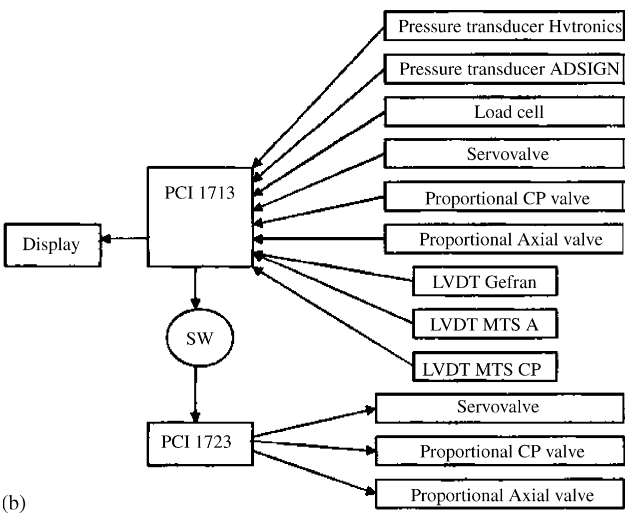

Fig. 18. System control using PCI 1713 and PCI 1723 for data acquisition and commands, reading and writing routes for sensors and actuators: (a) load cell and pressure transducers linking, (b) control diagram for the sensors and actuators.

The THF facility designed and constructed allowed for an accurate control into the necessary time demanded by a typical hydroforming work cycle. From the equivalence curves it was possible to program the parameters in order to obtain balanced axial displacements for the punch strokes.

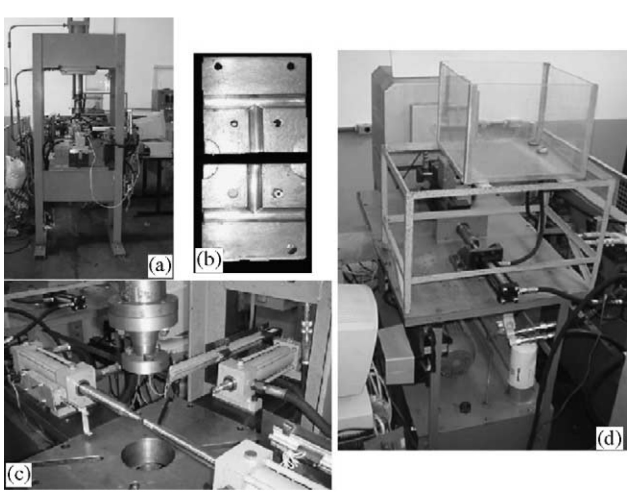

Fig. 19. THF facility (a) view of the complete THF press; (b) axial and counter pressure cylinders and theirs positions transducers; (c) die set cavities; (d) Pressure amplifier cylinders.

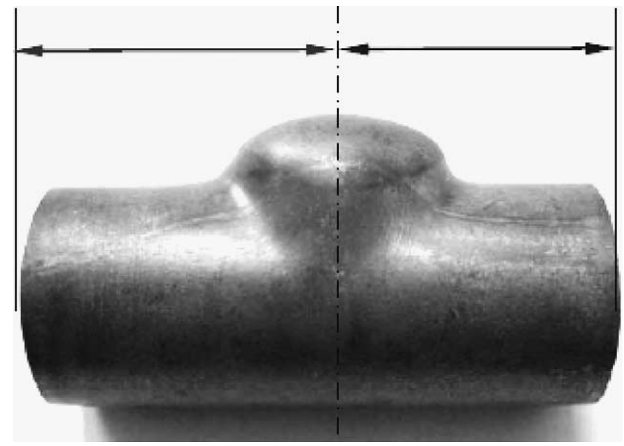

Fig. 20. THF part not centralized.

Future efforts will aim more deeply the study of spring back phenomena in hydroforming, specially the possibility of eliminate it, by the application and simultaneous control of the internal pressure and punch stroke, looking to avoid the

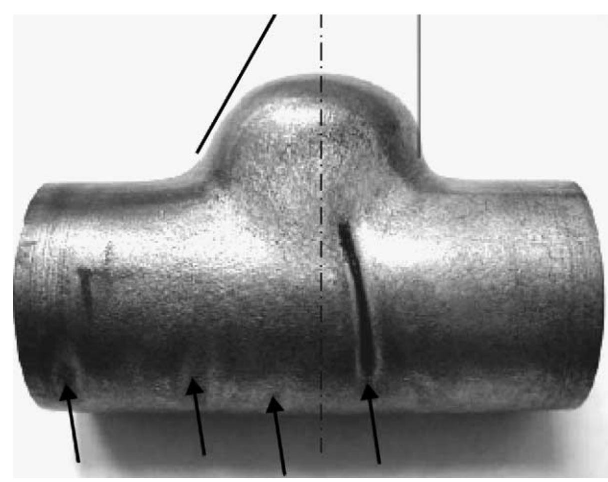

Fig. 21. THF part with wrinkling.

Fig. 22. THF part failure by buckling and fracture.

wrinkle formation and elimination of spring back generate trough them. In the end of the first step of this project, it could be concluded that the model generated using the LS-DYNA software as well as the FEA based on it, is mature and ready for the next tasks.

Acknowledgements

The authors acknowledge T-Systems do Brasil Ltda, for computational support and the software LS_DYNA. The support of UNIFEI for development of the THF facility is also gratefully acknowledged.

References

[1] M. Koç, T. Altan, An overall review of the tube hydroforming (THF) technology, J. Mater. Process. Technol. 108 (2001) 384–393.
[2] M. Ahmetoglu, T. Altan, Tube hydroforming: state-of-the-art and future trends, J. Mater. Process. Technol. 98 (2000) 25–33.
[3] G.F. Batalha, R.C. Schwarzwald, G.L. Damoulis, New trends in computer simulation as integrated tool for automotive components development, in: Proceedings of the Eighth Conference, NUMIFORM, Columbus, OH, 2004 (in CD).
[4] G. Morphy, The hydroforming design flexibility, The Tube Pipe J. (2002), http://www.thefabricator.com/xp/Fabricator/Articles/Esperts/.
[5] M. Imaninejad, G. Subhash, A. Loukus, Experimental and Numerical investigation of free-bulge formation during hydroforming of aluminum extrusions, J. Mater. Process. Technol. 147 (2004) 247–254.
[6] J.P. Abrantes, Simulação numérica via elementos finitos da conformação de chapas metálicas por pressure hidrostática (bulge test), Dissertação de mestrado, EPUSP, S. Paulo, Brazil, 2003 (in Portuguese).
[7] J.P. Abrantes, G.F. Batalha, Simulação numérica via elementos finitos da conformação de chapas metálicas por pressão hidráulica (bulge test), in: Congresso Brasileiro de Engenharia de Fabricação, vol. 2, COBEF, Uberlândia, ABCM, 2003.
[8] L.H. Lang, J. Danckert, K.B. Nielsen, Z.R. Wang, X.S. Wang, S. Yuan, Experimental and numerical investigation into useful wrinkling during aluminum alloy internal high-pressure forming, Proc. Inst. Mech. Eng. B: J. Eng. Manuf. 218 (2004) 43–49.
[9] M. Brunet, S. Boumaiza, G. Nefussi, Unified failure analysis for tubular hydroforming, J. Mater. Process. Technol. 149 (1–3) (2004) 217–225.
[10] Z.C. Xia, Failure analysis of tubular hydroforming, Trans. ASME-J. Eng. Mater. Technol. 123 (2001) 423–429.
[11] G. Nefussi, A. Combescure, Coupled buckling and plastic instability for tube Hydroforming, Int. J. Mech. Sci. 44 (2002) 899–914.
[12] J.O. Hallquist, LS-DYNA3D User's Manual, Version 940, Livermore Software Technology Corporation, 1997.
[13] R. Bortolussi, Análise Numérica e Experimental da Hidroconformação de Produtos Tubulares, Tese (Doutorado)-Universidade Estadual de Campinas/Faculdade de Engenharia Mecanica, Campinas, Brazil, 2001, 122 pp. (in Portuguese).
[14] A. Lejeune, N. Boudeau, J.C. Gelin, Influence of material and process parameters on the development of necking and bursting in flange and tube hydroforming, J. Mater. Process. Technol. 125/126 (2002) 849–855.
[15] A. Lejeune, N. Boudeau, J.C. Gelin, Influence of material and process parameters on bursting during hydroforming process, J. Mater. Process. Technol. 143/144 (2003) 11–17.
[16] B.J. MacDonald, M.S.J. Hashmi, Finite element simulation of bulge forming of a cross joint from a tubular blank, J. Mater. Process. Technol. 103 (2000) 333–342.
[17] P. Ray, B.J. MacDonald, Determination of the optimal load path for tube hydroforming processes using a fuzzy load control algorithm and finite element analysis, Finite Elements Anal. Des. 41 (2004) 173–192.
[18] http://nsmwww.eng.ohiostate.edu/THF_Automotive_Appln_Dr_G_Mississipi.pdfr.
[19] N. Asnafi, Analytical modeling of tube hydroforming, Thin Walled Struct. 34 (1999) 295–330.
[20] N. Asnafi, A. Skogsgardh, Theoretical and experimental analysis of stroke-controlled tube hydroforming, Mater. Sci. Eng. A 279 (2000) 95–110.
[21] A. Szabo-Ponce, G.F. Batalha, Conformação hidrostática de chapas e tubos, in: VI Conferência nacional de conformação de chapas, Porto Alegre, UFRGS, 2003, pp. 165–176.
[22] A. Szabo-Ponce, G.F. Batalha, Controle do processo de conformação hidrostática de chapas e tubos, in: VII Conferência nacional de conformação de chapas, Porto Alegre, Brazil, UFRGS, 2004, 2003, pp. 155–166 (in Portuguese).
[23] A. Szabo-Ponce, R. Bortolussi, G.F. Batalha, Hidroconformação de Tubos: Influência dos parâmetros no processo, Submitted to the III Brazilian Meeting on Manufacturing Engineering, to be held in Joinville, Brazil.